First principles 3D simulation of tokamak plasma breakdown

J. Chew[1], P. Gibbon[1], D. Brömmel[1], P. C. De Vries[2], Y. Gribov[2]

[1] *Jülich Supercomputing Centre, Forschungszentrum Jülich GmbH, 52425 Jülich, Germany*

[2] *ITER Organization, Route de Vinon sur Verdon, 13067 St. Paul Lez Durance, France*

The growth rate of the ionisation fraction f_i in tokamak start up via the Townsend avalanche process is often described by a simplified zero dimensional (0D) model [1],

$$\frac{1}{f_\mathrm{i}}\frac{\mathrm{d}f_\mathrm{i}}{\mathrm{d}t} = \alpha V_\mathrm{De} - \frac{V_\mathrm{De}}{L}; \quad V_\mathrm{De} \sim 5730\frac{E}{p}. \tag{1}$$

where $\alpha(E,p)$ is the first Townsend coefficient as a function of the toroidal electric field strength E and gas fill pressure p, V_De is the electron drift velocity, and L the connection length. The proposed approximation of the V_De originates from the assumption that the electron acceleration due to electric fields will eventually reach an equilibrium with the collisional drag which causes V_De to settle on a constant value with the given E and p. This work studies the Townsend avalanche process with a fully resolved kinetic model in a three dimensional toroidal geometry along with prescribed electric and magnetic fields. The goal is to accurately determine key breakdown characteristics such as ionisation fraction over time and the resulting mean electron drift velocity V_DE, thus comparing the results with 0D model given in Eq. 1. The first-principles method also provides new insight into the charge velocity and spatial distribution in the very early stages of plasma initiation, as well as electron loss over time.

The simulation domain is a simple torus with major radius of 5.8 m and minor radius of 1.0 m, which resembles the breakdown volume of the ITER tokamak. Throughout the simulation, any charged particles that ventured further than minor radius of 1.75 m will be treated as runaway charges. The simulation is then initiated with a H_2 gas pressure of 2 mPa, subjecting the initially seeded 1000 electrons to a toroidal electric field of $0.6\,\mathrm{V\,m^{-1}}$ at the magnetic null (which coincides with the torus' major radius). The simulation is expected to have a higher ionisation growth rate than ITER's approximate operating conditions, since the chosen electric field strength and neutral gas pressure are twice the magnitude while giving an E/p of $300\,\mathrm{V\,m^{-1}\,Pa^{-1}}$. The prescribed toroidal and poloidal magnetic field, as well as the toroidal magnetic field are shown in Fig. 1. A simplification is made that the poloidal field coils can

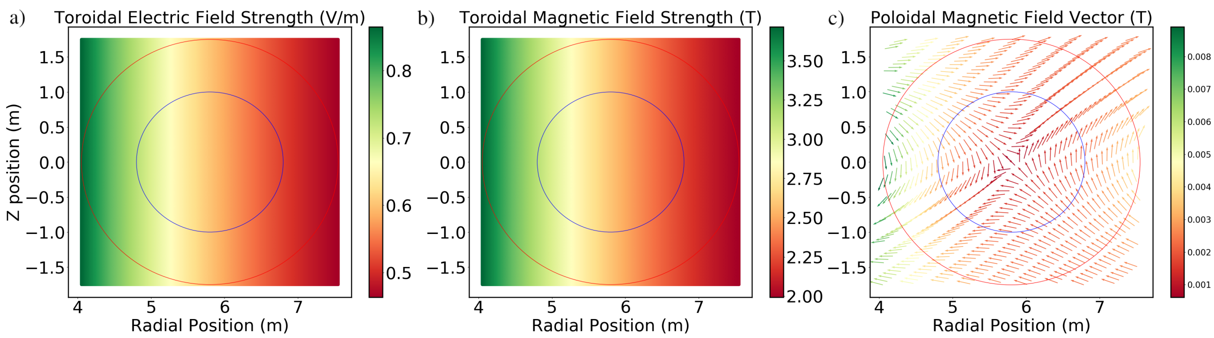

Figure 1: Both toroidal electric and magnetic field are aligned and pointing outward from the figure. The blue circle shows the area where initial electrons are seeded and the red circle indicates the extent of the simulated domain. Particles that cross the red boundary are counted as runaway charges and are not simulated further.

be represented by a set of four current loops, obtaining the poloidal magnetic field by solving Biot-Savart's law. Positions of the loops and their current magnitudes are chosen such that a magnetic null is formed at a location which coincides with the torus' major radius. A perturbation of approximately 5×10^{-4} T is also added to the poloidal magnetic field which mimics the slight imperfections encountered in an actual tokamak device.

Each of the charged particles is individually followed throughout the simulation, resolving their gyromotion in the prescribed fields with a time step size of 17.5 ps. Electrostatic potentials are computed via a mesh-free Coulomb solver which is a parallel implementation of Barnes-Hut tree traversal algorithm and the Random Scatter model is chosen to resolve electron-neutral collision events [2]. The considered cross sections are:

- $e + \mathrm{H}_2 \to e + \mathrm{H}_2$ (elastic scattering)
- $e + \mathrm{H}_2 \to e + \mathrm{H}_2^*$ (inelastic scattering)
- $e + \mathrm{H}_2 \to e + 2\mathrm{H}$ (neutral dissociation)
- $e + \mathrm{H}_2 \to 2e + \mathrm{H}_2^+$ (nondissociative ion.)
- $e + \mathrm{H}_2 \to 2e + \mathrm{H} + \mathrm{H}^+$(dissociative ion.)
- $e + \mathrm{H}_2 \to e + \mathrm{H} + \mathrm{H}^*$ (neutral dissociation)

It can be observed from Fig. 2a that the growth rate of free electrons in the three dimensional simulation outpaces the prediction by the zero dimensional model. This is due to excessive collisional drag in the zero dimensional model (thus an underestimation of the V_{De}) since the velocity vector of scattered electrons is assumed to be either parallel or anti-parallel along the direction of acceleration. This causes an underestimation of the ionisation rate and subsequently a lower electron growth rate compared to the simulation in three dimensional space and momentum. Fig. 2b details the recorded counts for the various simulated particle species. The first instance of lost electrons (which leave the simulated domain) is recorded at approximately 0.27 ms. Referring to Fig. 3a, there are a total of 137 342 electrons present in the simulation at 0.48 ms. 336 electrons carry energy of more than 1 keV and will soon leave the simulated domain (due to diminishing cross sections that can impede continuous energy gain). The electron loss rate at least up to 0.5 ms appears to have little effect on the electron growth rate from impact ionisation. This balance between electron losses and ionisation growth still needs to be verified beyond several milliseconds in order to assess whether the Townsend avalanche breakdown can be sustained

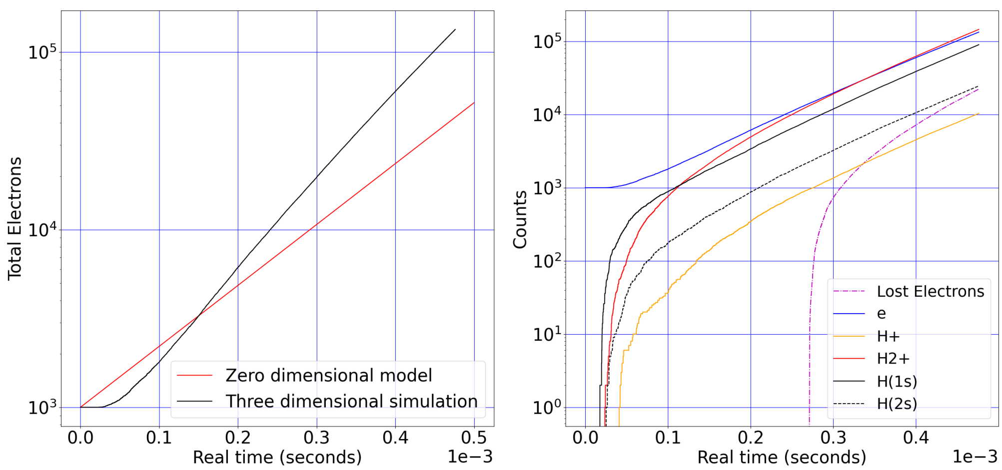

Figure 2: a) Comparison of total electron counts over time. b) Particle counts over time in simulation, lost electrons included.Townsend breakdown avalanche in an ITER-sized tokamak is expected to last around 20 ms.

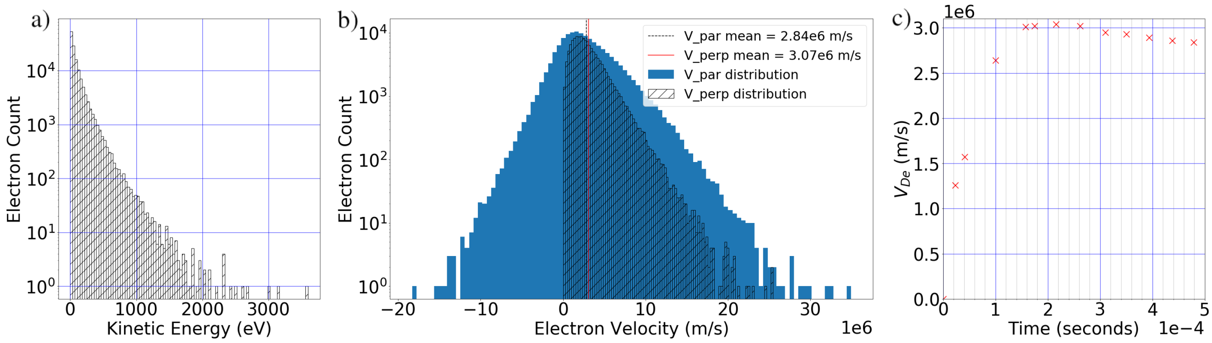

Figure 3: a) Energy distribution of electrons. b) Velocity distribution of electrons, in both parallel and perpendicular with respect to the toroidal direction. Measured at 0.48 ms.

towards the completion of burn-through phase.

In order to have a meaningful comparison of the drift velocity from Eq. 1 with the velocity computed in a three dimensional simulation, only the velocity component parallel to the toroidal direction is considered. With a chosen E/p of 300 $\mathrm{V\,m^{-1}\,Pa^{-1}}$, the zero dimensional model predicts a V_{De} of $1.72 \times 10^6\,\mathrm{m\,s^{-1}}$ [1]. Fig. 3b shows that the average electron drift velocity parallel to the toroidal direction at 0.48 ms is $2.84 \times 10^6\,\mathrm{m\,s^{-1}}$, which is 65% higher than the predicted value. This is related to the excessive collisional drag in the zero dimensional model explained earlier. Interestingly, we observe that the average velocity perpendicular to the toroidal direction is of the same order of magnitude as the parallel counterpart, an effect which of course cannot be taken into account in the zero dimensional model. Referring to Fig. 3c, it can be seen that V_{De} peaks at approximately $3 \times 10^6\,\mathrm{m\,s^{-1}}$ at 0.22 ms before decreasing somewhat from approximately 0.27 ms, coinciding with the onset of electron loss.

Observing the spatial distribution of electrons over time (Fig. 4a-c) reveals that the poloidal magnetic field strongly impacts the location of plasma formation in the poloidal plane. It can be seen in Fig. 4a that although the initial seeding of the electrons is made randomly in a uniform manner along the torus, the electrons are slowly driven away diagonally from the magnetic null towards the top left and bottom right corners, eventually adding a sparse cloud structure on the right-hand side. Comparing with Fig. 4d, this corresponds to regions in which the magnitude of the poloidal magnetic field's angular component is lowest. Another interpretation is that those areas are where the poloidal magnetic field vectors are mostly aligned to the radial component, pointing inward (or outward) from the magnetic null. As such, the electron drift motion in the poloidal plane encounters least resistance radially along the 'valley'. Further study of the drift in the poloidal direction due to the interplay between magnetic field geometry and electron-neutral scattering is required to better explain the formation of this cloud structure.

The total current density from all simulated charges is shown in Fig. 5. The areas which recorded high current density naturally corresponds to the charge concentration displayed in Fig. 4, and the higher magnitude in areas closer to the inner side of the torus is a direct consequence of the toroidal electric field gradient shown in Fig. 1a. In Fig. 5, the maximum recorded current density in the slice aligned along the X-Z plane is $2.88 \times 10^{-8}\,\mathrm{A\,m^{-2}}$ with the diagnostic cell area of $3 \times 10^{-3}\,\mathrm{m^2}$. Taking the measurement over the entire circular area with radius of 1.75 m yields a current density of $4 \times 10^{-6}\,\mathrm{A\,m^{-2}}$. While the measured current density will grow exponentially over time, it is clear that 0.48 ms is still in the very early stage of plasma initiation. In fact, at this point the measured current density is approximately 10 orders of mag-

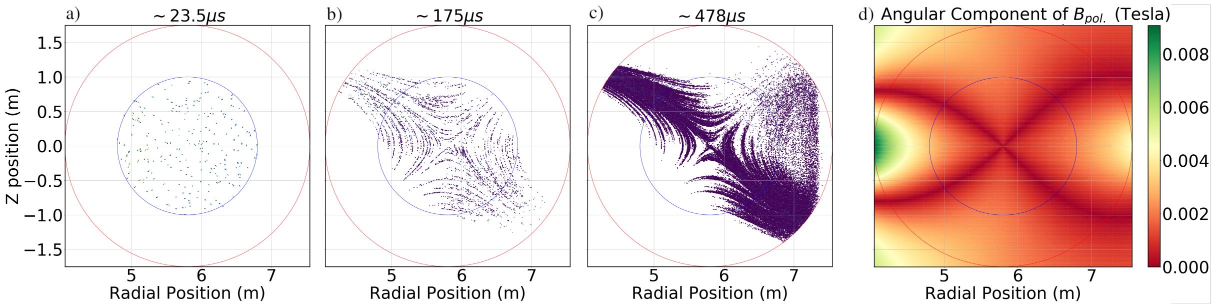

Figure 4: a) - c) Time evolution of the electron spatial distribution, projected onto the poloidal plane. d) Magnitude of angular component of the poloidal magnetic field (T).

nitude lower compared to the $1.5\,\mathrm{kA\,m^{-2}}$ expected in ITER during the avalanche phase. Thus, the self-generated poloidal magnetic field from the computed current is far below the threshold required to form closed magnetic flux surfaces, considering that the prescribed poloidal magnetic field has perturbations of $5 \times 10^{-4}\,\mathrm{T}$.

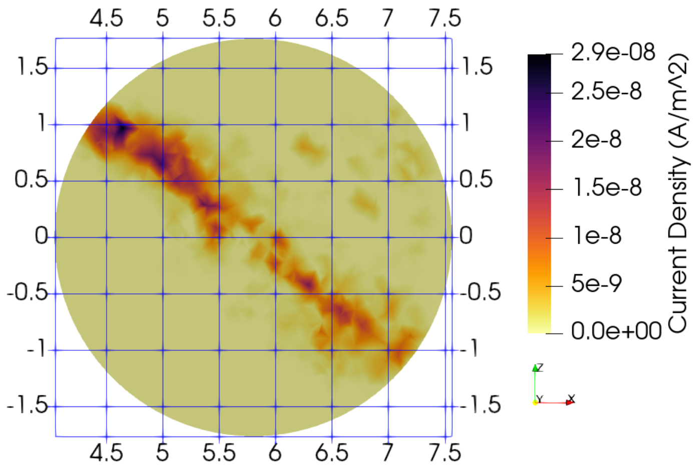

Figure 5: Computed current density at 0.48 ms.

In summary, a first principles three dimensional simulation of the plasma initiation phase in an ITER-like tokamak has been made which shows that the zero dimensional model probably underestimates the ionisation growth rate. The influence of prescribed poloidal magnetic fields on regions of plasma formation during the very early breakdown phase is revealed by the emergence of a highly non-uniform electron spatial distribution in poloidal plane. The zero-dimensional model predicts that the charged particle number density should reach $1 \times 10^{15}\,\mathrm{m^{-3}}$ at 3.5 ms, at which point the resulting current is strong enough to create self-generated poloidal magnetic fields exceeding the prescribed field strength. An immediate outlook of this study is to extend the simulation over several ms to verify that the ionisation growth rate is sustained despite losses, and to investigate localised early formation of closed magnetic flux surfaces.

Acknowledgment

The authors gratefully acknowledge the computing time granted through JARA on the supercomputer JURECA at Forschungszentrum Jülich.

References

[1] P.C. de Vries and Y. Gribov, *Nuclear Fusion* **59** 096043 (2019)
[2] J. Chew *et al*, *Plasma Phys. Control. Fusion* **63** 045012 (2021)